Combination Radiofrequency Ablation and Intravenous Radiolabeled Liposomal Doxorubicin: Imaging and Quantification of Increased Drug Delivery to Tumors[1]

Hayden W. Head, MD
Gerald D. Dodd III, MD
Ande Bao, PhD
Anuradha Soundararajan, PhD
Xavier Garcia-Rojas, MD
Thomas J. Prihoda, PhD
Linda M. McManus, PhD
Beth A. Goins, PhD
Cristina A. Santoyo, MS
William T. Phillips, MD

© RSNA, 2010

Purpose: To identify, with noninvasive imaging, the zone of radiopharmaceutical uptake after combination therapy with radiofrequency (RF) ablation and intravenous administration of technetium 99m (^{99m}Tc) liposomal doxorubicin in a small-animal tumor model, and to quantify and correlate the uptake by using imaging and tissue counting of intratumoral doxorubicin accumulation.

Materials and Methods: This study was approved by the animal care committee. Two phases of animal experiments were performed. In the first experiment, a single human head-and-neck squamous cell carcinoma tumor was grown in each of 10 male nude rats. Seven of these animals were treated with intravenous ^{99m}Tc–liposomal doxorubicin followed by RF tumor ablation at a mean temperature of 70°C ± 2 for 5 minutes, and three were treated with intravenous ^{99m}Tc–liposomal doxorubicin only. Combination single photon emission computed tomography–computed tomography (SPECT/CT) was performed at 15 minutes, 4 hours, and 20 hours after therapy. In the second experiment, two tumors each were grown in 11 rats, but only one of the tumors was ablated after intravenous administration of ^{99m}Tc–liposomal doxorubicin. SPECT/CT and planar scintigraphy were performed at the same posttreatment intervals applied in the first experiment, with additional planar imaging performed at 44 hours. After imaging, tissue counting in the excised tumors was performed. Radiotracer uptake, as determined with imaging and tissue counting, was quantified and compared. In a subset of three animals, intratumoral doxorubicin accumulation was determined with fluorimetry and correlated with the imaging and tissue-counting data.

Results: At both SPECT/CT and planar scintigraphy, increased uptake of ^{99m}Tc–liposomal doxorubicin was visibly apparent in the ablated tumors. Results of quantitative analysis with both imaging and tissue counting confirmed significantly greater uptake in the RF ablation–treated tumors ($P < .001$). Intratumoral doxorubicin accumulation correlated closely with imaging ($r = 0.9185$–0.9871) and tissue-counting ($r = 0.995$) results.

Conclusion: Study results show that increased delivery of intravenous liposomal doxorubicin to tumors combined with RF ablation can be depicted and quantified with noninvasive imaging.

©RSNA, 2010

Supplemental material: *http://radiology.rsna.org/lookup /suppl/doi:10.1148/radiol.10090714/-/DC1*

Radiofrequency (RF) ablation and other thermal therapies are increasingly being used for focal tumor therapy in various organs, including the liver (1–3), kidneys (4,5), lungs (6), bone (7,8), and breasts (9,10). Clinical study results have shown limitations of these therapies in larger tumors and suggest incomplete treatment, especially at the tumor margins (1–5,9). Methods to overcome this limitation have been explored in research. Prior work has revealed the potential usefulness of combining thermal therapies with intravenous and intraarterial chemotherapy to facilitate increased tumor necrosis (11–24), reduced tumor growth, and/or increased local tumor control (22,25–31). Furthermore, increased drug deposition has been observed, particularly in the tumor tissue surrounding the primary ablation zone (16–18,32). The drug deposition patterns in combination therapies have thus far been characterized by using invasive methods such as histopathologic analysis and drug extraction and quantification. Therefore, the next necessary step is to identify a method of noninvasively imaging drug deposition in combination with RF ablation. The purpose of this study was to identify, with noninvasive imaging, the zone of radiopharmaceutical uptake after combination therapy with RF ablation and intravenously administered technetium 99m ($99m$Tc) liposomal doxorubicin in a small-animal tumor model, and to quantify and correlate the uptake by using imaging and tissue counting of intratumoral doxorubicin accumulation.

Materials and Methods

Animal and Tumor Model

All authors had control of the study data. The experiments performed in this study were approved by the animal care committee of the University of Texas Health Science Center at San Antonio and were compliant with National Institutes of Health animal care guidelines (33). During all procedures, the animals were anesthetized with 1%–3% isoflurane (IsoSol; VedCo, St Joseph, Mo) in 100% oxygen with use of an anesthesia inhalation unit (Vapomatic; A.M. Bickford, Wales Center, NY).

Experiments were performed in 28 athymic nude male rats (Hsd:RH-*Foxn1^{rnu}*; Harlan, Indianapolis, Ind) by using human head-and-neck squamous cell carcinoma (SCC) xenografts, as previously characterized by Bao et al (34). Cells from an established human tongue SCC cell line (SCC-4; American Type Culture Collection, Manassas, Va) were inoculated subcutaneously into one or two locations: In 14 rats, the SCC cell line was injected into the midline of the neck dorsum. In 14 additional rats, two inoculations each were performed on either side of the base of the neck. Each inoculation contained 5×10^6 SCC-4 cells in 0.20 mL of saline. The target tumor volume for these experiments was 1.5 cm^3. According to previous characterization of the growth of this tumor (34), this size should be achieved 13 days after inoculation.

Radiolabeling Procedure

The procedure for labeling liposomal doxorubicin with $99m$Tc included two steps (35): First, $99m$Tc–N,N-bis(2-mercaptoethyl)-N',N'-diethylethylenediamine (BMEDA) was prepared in our laboratory (36). Second, $99m$Tc-BMEDA was used to label 2 mL of commercially available liposomal doxorubicin (Doxil; Ortho Biotech, East

Advances in Knowledge

- The increased delivery of liposomal doxorubicin to tumors—when this agent is administered intravenously in combination with radiofrequency (RF) ablation—can be depicted and quantified with noninvasive imaging.
- Both combination single photon emission computed tomography–computed tomography and planar scintigraphy can depict the increased uptake of technetium 99m ($99m$Tc) liposomal doxorubicin in ablated tumors.
- The results of quantitative analysis with tissue counting and both imaging modalities confirmed the significantly greater uptake of $99m$Tc–liposomal doxorubicin in RF-ablated tumors.
- Intratumoral doxorubicin accumulation correlated closely with the $99m$Tc activity measured with imaging and tissue counting.

Implications for Patient Care

- Combination thermal ablation–radiolabeled liposomal doxorubicin chemotherapy may be able to potentiate the treatment of solid cancers in human patients by means of increased drug delivery.
- It also may be a useful means of noninvasively assessing treatment response over time with multimodality imaging.
- Potential chemodosimetry of liposomal drugs with use of noninvasive imaging methods may yield prognostic information regarding the success of tumor treatment and the necessity of repeat treatment.

Bridgewater, NJ) by means of incubation at 37°C for 1 hour. The resultant [99mTc]-doxorubicin liposomes were separated from unencapsulated [99mTc]-BMEDA by way of disposable columns (Sephadex G-25; GE Healthcare Bio-Science, Uppsala, Sweden) and eluted with phosphate-buffered saline at a pH of 7.4.

Experimental Design

The study consisted of two phases. Phase 1 was performed in animals bearing a single subcutaneous tumor. In phase 2, each animal had two tumors. Both phases were designed to study the effect of combined RF ablation–intravenous [99mTc]–liposomal doxorubicin therapy.

Phase 1: single-tumor model.—A total of 14 rats (14 tumors) were included. The tumors in one cohort of seven rats were treated with RF ablation within 5 minutes after the intravenous administration of [99mTc]–liposomal doxorubicin (Fig 1a). A second cohort of three rats were treated with intravenous [99mTc]–liposomal doxorubicin only. A third set of four control rats were treated with RF ablation only.

Phase 2: two-tumor model.—A total of 14 rats (28 tumors) were included. In 11 of these animals, one of the two tumors was treated with RF ablation within 5 minutes after the intravenous administration of [99mTc]–liposomal doxorubicin (Fig 1b). The nonablated tumor served as a same-animal control. In three additional control animals, one of the two tumors was treated with RF ablation but no intravenous drug administration.

[99mTc]–Liposomal Doxorubicin Administration

Liposomal doxorubicin labeled with [99mTc] was administered via a tail vein. Each dose was formulated to provide 6.5 mg of doxorubicin and 52 mg of lipid per kilogram of body weight. The clearance of [99mTc]–liposomal doxorubicin is biphasic, with half clearance times of 2.2 and 26.2 hours in normal rats. The amount of injected [99mTc]–liposomal doxorubicin remaining in the circulation is approximately 50% at 13 hours and 20% at 44 hours (35). These values are similar to those reported for nonlabeled liposomal doxorubicin (37).

Tumor Ablation

RF ablation was performed with a specialized 21-gauge non–internally cooled straight-needle electrode with a 1-cm exposed tip. The electrode was powered by a 500-kHz, 200-W RF generator (CC-1; Valleylab [now Covidien], Boulder, Colo). To complete the electrical circuit, the animal was placed on a standard grounding electrode (Valleylab), with contact ensured by using electrolytic gel. Because of the subcutaneous location of the tumor, the needle tip was easily placed in the center of the tumor by means of visualization and palpation. RF energy was applied for 5 minutes at a mean temperature of 70°C ± 2. This ablation protocol was adapted from previously published animal studies (11–13,16–18,26,32).

Imaging Protocol

For all animals that received an intravenous [99mTc]–liposomal doxorubicin injection, fused single photon emission computed tomographic and computed tomographic (SPECT/CT) images were obtained at three time points after the injection (15 minutes, 4 hours, and 20 hours) by using a dual-modality system (X-SPECT/CT; Gamma Medica, Northridge, Calif). SPECT projection data were acquired by using a 56 × 56 image matrix size with dual gamma cameras equipped with low-energy parallel hole collimators for 32 projections, at 20 seconds per projection for the 15-minute and 4-hour time points and at 40 seconds per projection for the 20-hour time point. CT data were acquired at a voltage of 75–80 kVp and at a tube current of 0.25 mA in the fly mode and were reconstructed to form a volumetric image in a 512 × 512 × 512 matrix size by using a reconstruction algorithm provided by the camera manufacturer. In addition, in phase 2, anterior and posterior planar scintigraphic images were obtained at the same time points (1-minute image acquisition time for the 15-minute and 4-hour time points, 3-minute image acquisition for the 20-hour time point) and at 44 hours (10-minute image acquisition) after the [99mTc]–liposomal doxorubicin injection by using the two gamma cameras of the same system.

Figure 1

a.

b.

Figure 1: Experimental setup of single- and two-tumor models. **(a)** RF ablation needle electrode is inserted into a single-tumor xenograft (arrow) in the back of the neck of a nude rat. A ground electrode covered in aluminum foil is placed underneath the rat. **(b)** RF ablation needle electrode is inserted into one of two tumor xenografts (arrowhead and arrow) on either side of the base of the neck.

Image Analysis

SPECT/CT images were reconstructed as three-dimensional images and assessed at manual volumetric region-of-interest analysis by using Amira 3.1 computer software (TGS, San Diego, Calif). Manually drawn regions of interest on planar images were analyzed by using ASIPro VM software (Concorde Microsystems, Knoxville, Tenn), with the geometric mean of the counts obtained from the anterior and posterior images taken into account.

Tissue Counting

For all animals that received intravenous ^{99m}Tc–liposomal doxorubicin, the radioactivity of all excised tumors was quantified by using a gamma well counter (Wallac 1480 WIZARD; Perkin-Elmer, Boston, Mass). The percentages of injected ^{99m}Tc activity per whole tumor and per gram of tumor tissue were calculated by using a previously described method (35).

Gross Pathologic and Histopathologic Analyses

After being imaged, the rats were euthanized by means of pentobarbital-phenytoin (Euthasol; Virbac Animal Health, Fort Worth, Tex) overdose and cardiac exsanguination while still anesthetized. Their tumors were excised, weighed, and measured with calipers. With the exception of the tumors in three rats that received the combination treatment in the phase 2 experiments and were used for doxorubicin quantification, which were not sectioned, the tumors in all animals were sectioned perpendicular to the needle track into 2–3-mm slices. The tumor slices were bathed in 2% triphenyltetrazolium chloride (Sigma, St Louis, Mo) for 30 minutes. With this method, viable tissue with intact mitochondrial activity stains red and there is no staining of ablated tissue, which indicates irreversible cellular injury (38). Gross-specimen caliper measurements were performed independently in a masked fashion by two investigators (H.W.H., A.B.). The maximal diameter of the nonstained zone perpendicular to the needle track was considered the ablation size. For histo-

pathologic analysis, hematoxylin-eosin staining and subsequent examination with light microscopy were performed on specimens from representative tumors in each group.

Doxorubicin Quantification

For three animals used in the phase 2 experiments, the six excised tumors (two tumors each from three rats) were not studied at pathologic analysis after ^{99m}Tc measurement; rather, they were frozen at –20°C. These tumors were homogenized in acid alcohol (0.3N hydrochloric acid, 70% ethyl alcohol), and doxorubicin was extracted for 24 hours at 4°C. Aliquots of extracted samples were pipetted into a 96-well microplate. To quantify doxorubicin, fluorimetry was performed with a microplate reader (BioTek, Winooski, Vt) at an excitation wavelength of 470 nm and an emission wavelength of 590 nm by using a standard curve of doxorubicin concentrations ranging from 0.0 to 0.05 mg/mL (16,17,32).

Statistical Analysis

For the phase 1 and phase 2 experiments, radiotracer uptake was compared at SPECT/CT image analysis and mixed-model analysis of variance (ANOVA) for repeated measures, with subsequent multiple comparisons performed by using the ANOVA error term. Ablation status (ablated versus nonablated tissue) was the between-subject factor, and time after injection was the within-subject factor. Model assumptions of homogeneity of variance and bell-shaped distribution were examined to ensure valid analyses. These criteria were better met by using the standard logarithmic transformation of the raw data. The same method was used to compare radiotracer uptake at planar scintigraphic analysis in the phase 2 experiments. For phase 1, unpaired t tests were used to compare the radiotracer uptake measured according to tissue count and gross ablation size in all 10 animals (10 tumors) treated with ^{99m}Tc–liposomal doxorubicin. For phase 2, paired t tests were used to compare the radiotracer uptake measured with tissue counting in 11 animals.

One-way ANOVA was used to compare the gross ablation sizes between all groups.

Linear regression and Pearson correlation analyses were used to characterize the relationship between the quantity of doxorubicin extracted from the tumors and the corresponding data obtained at image analysis and tissue counting. All reported P values were calculated by using two-sided tests. $P < .05$ was considered to indicate a significant difference. Statistical analyses were performed by using statistical computer software (SAS, release 9.1, SAS Institute, Cary, NC; Prism 5, version 5.01, GraphPad Software, San Diego, Calif; and Excel 2007, Microsoft, Redmond, Wash).

Results

Radiolabeling

The mean initial ^{99m}Tc activity was 1.5 GBq ± 0.3 (standard deviation) (range, 1.1–1.9 GBq), and the mean labeling efficiency was 64.7%. The mean ^{99m}Tc activity injected per rat was 0.23 GBq ± 0.05 (range, 0.18–0.36 GBq). The mean volume of ^{99m}Tc–liposomal doxorubicin injected per rat was 2.0 mL ± 0.3 (range, 1.6–2.5 mL), with a mean lipid dose per injection of 12.1 mg ± 2.0 (range, 8.3–15.9 mg).

Imaging and Tissue Counting Analyses

One rat used in phase 2 was excluded from SPECT/CT image analysis owing to faulty image acquisition 15 minutes after ^{99m}Tc–liposomal doxorubicin administration. Another rat in phase 2 was excluded from planar image analysis because it died before the 44-hour acquisition.

A visually striking increase in ^{99m}Tc–liposomal doxorubicin accumulation was observed in all of the tumors (those in the rats used in both phases) treated with combination therapy; the increased uptake was readily apparent at both SPECT/CT and planar scintigraphy at all time points (Fig 2a, 2b). A three-dimensional reconstructed SPECT/CT image obtained in the two-tumor model also demonstrates this difference (Movie [online]). Analysis of the SPECT/CT
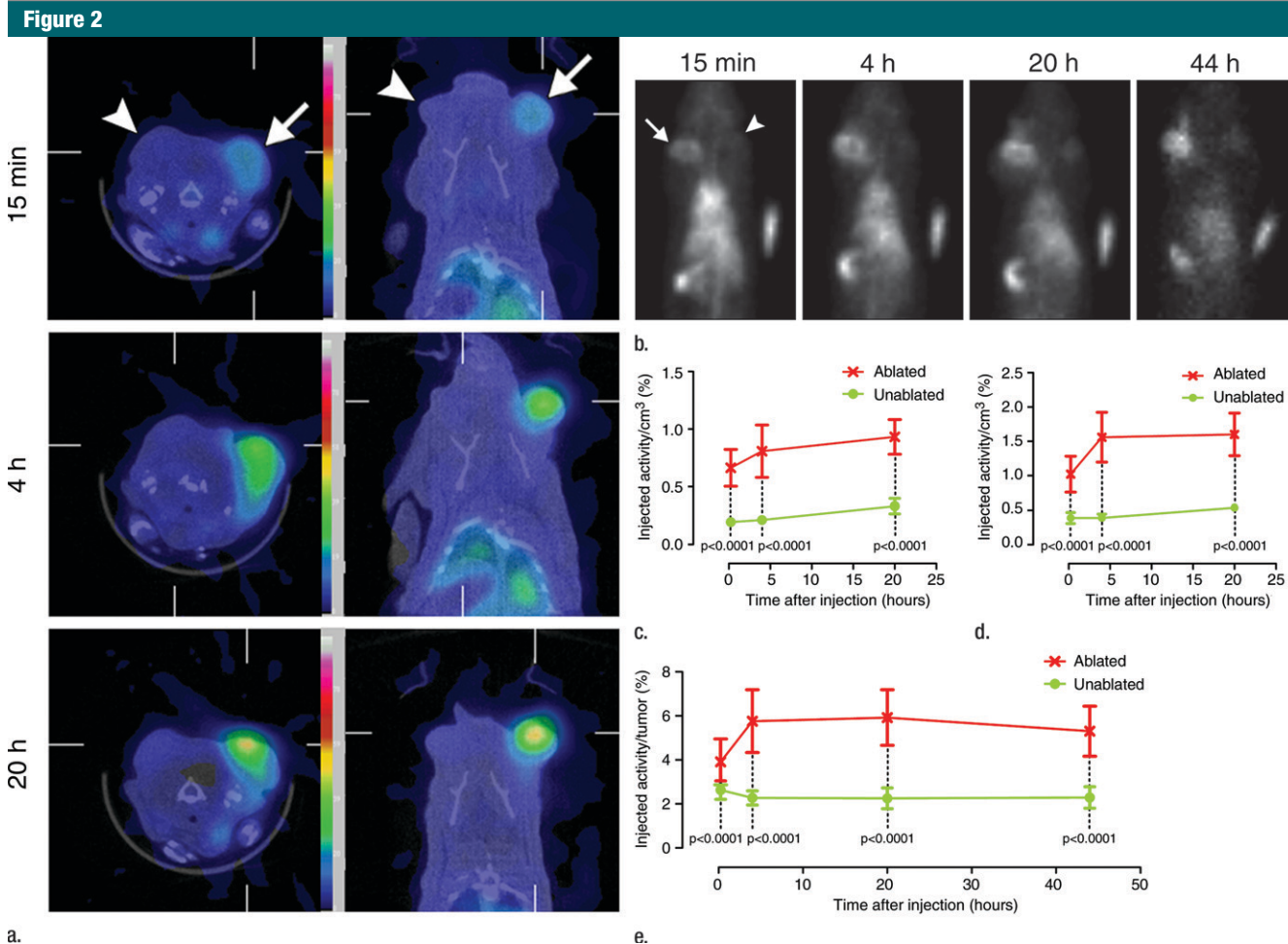
Figure 2

Figure 2: Increased uptake of ^{99m}Tc–liposomal doxorubicin in RF-ablated tumors. **(a)** Transaxial (left) and coronal (right) SPECT/CT images acquired at three time points after intravenous administration of ^{99m}Tc–liposomal doxorubicin in rat with two tumors. Right tumor (arrows) was also treated with RF ablation. Left tumor (arrowheads) was not ablated. Color map represents SPECT pixel values from 0 to an arbitrary maximal value of 100, indicating percent relative ^{99m}Tc activity. **(b)** Posterior scintigraphic images acquired at four time points after intravenous administration of ^{99m}Tc–liposomal doxorubicin in different rat with two tumors. Left tumor (arrow) was also treated with RF ablation. Right tumor (arrowhead) was not ablated. **(c)** Graph illustrates percentages of injected ^{99m}Tc activity per cubic centimeter of tumor tissue at three time points, as determined at SPECT/CT analysis of single tumors in seven rats treated with combined RF ablation–intravenous ^{99m}Tc–liposomal doxorubicin and three rats treated with intravenous ^{99m}Tc–liposomal doxorubicin only. **(d)** Graph illustrates percentages of injected ^{99m}Tc activity per cubic centimeter of tumor tissue at three time points, as determined at SPECT/CT analysis of rats with two tumors each, one of which was treated with RF ablation after intravenous ^{99m}Tc–liposomal doxorubicin. **(e)** Graph illustrates percentages of injected ^{99m}Tc activity per whole tumor at four time points, as determined at scintigraphic analysis of rats with two tumors each, one of which was treated with RF ablation after intravenous ^{99m}Tc–liposomal doxorubicin. In **c–e**, center points indicate means and error bars indicate 95% confidence intervals. *P* values were calculated at two-way ANOVA after logarithmic transformation of raw data.

and planar images revealed significant differences in ^{99m}Tc–liposomal doxorubicin uptake at all time points, with an initial sharp increase (Fig 2c–2e). For all animals that received intravenous ^{99m}Tc–liposomal doxorubicin, these imaging findings were confirmed with tissue counting in terms of percentage accumulation of injected radiotracer dose per whole tumor and per gram of tumor tissue (Table 1).

Gross Pathologic Analysis

For the rats used in phase 1, the mean tumor weight and mean tumor diameter were 3.19 g ± 1.12 (range, 1.98–5.94 g) and 16.9 mm ± 2.4 (range, 14.4–22.2 mm), respectively. For the animals used in phase 2, the mean tumor weight and mean tumor diameter were 2.07 g ± 1.28 (range, 0.40–5.72 g) and 13.8 mm ± 3.2 (range, 8.0–20.0 mm), respectively. At gross-specimen inspection and dissection, the ablation zones in the tumors treated with RF ablation, with or without ^{99m}Tc–liposomal doxorubicin, had well-demarcated nonstained areas, which

Table 1

^{99m}Tc–Liposomal Doxorubicin Uptake Measured with Tissue Counting

Study Phase and Tumor Model*	Ablated Tumors[†]	Nonablated Tumors[†]	P Value
Phase 1: single-tumor model			
Per whole tumor	2.148 ± 0.625 (1.186–3.147)	0.842 ± 0.225 (0.706–1.103)	.009
Per gram of tumor tissue	0.891 ± 0.251 (0.624–1.327)	0.388 ± 0.056 (0.326–0.434)	.011
Phase 1: two-tumor model			
Per whole tumor	2.264 ± 0.850 (0.927–4.052)	1.086 ± 0.539 (0.329–1.953)	<.001
Per gram of tumor tissue	1.961 ± 0.576 (0.627–2.727)	0.833 ± 0.238 (0.443–1.138)	<.001

* In phase 1 of this study, unpaired *t* tests were used to compare radiotracer uptake measured at tissue counting between seven rats (seven tumors) treated with ablation and three rats (three tumors) not treated with ablation. In phase 2, paired *t* tests were used to compare radiotracer uptake measured with tissue counting between the RF-ablated and non–RF-ablated tumors in the same 11 rats.

[†] Data are mean uptake values (in percentage) ± standard deviations, with ranges in parentheses.

Table 2

Gross-Specimen Ablation Zone Sizes

Tumor-Treatment Group	No. of Tumors	Mean Ablation Size (mm)*
Single-tumor model, combination therapy	7	10.2 ± 1.9 (6.9–12.7)
Single-tumor model, RF ablation only	4	11.0 ± 1.5 (8.9–12.2)
Single-tumor model, ^{99m}Tc–liposomal doxorubicin only	3	NM
Two-tumor model, combination therapy	8	10.2 ± 1.6 (8.1–12.3)
Two-tumor model, RF ablation only	3	11.3 ± 1.1 (10.0–12.1)
Two-tumor model, ^{99m}Tc–liposomal doxorubicin only	8	NM

Note.—Combination therapy refers to RF ablation combined with intravenous ^{99m}Tc–liposomal doxorubicin therapy. In the single- and two-tumor models, the tumors treated with RF ablation only were considered controls. NM = not measurable.

* Data are means ± standard deviations, with ranges in parentheses.

represented ablation zones (Fig 3). There was no significant difference in ablation zone size between the tumors treated with combination therapy and those treated with ablation only ($P = .735$, ANOVA) (Table 2).

Histopathologic Analysis

Histopathologic examination findings showed the ablated tumors to have focal thermal injury changes that were absent in the nonablated tumors (Fig 4). The ablated tumors had a confluent central zone of necrotic debris. There was no discernable difference between the ablated tumors treated with and those treated without intravenous ^{99m}Tc–liposomal doxorubicin administration. The nonablated tumors showed nests and cords of intact, viable tumor cells encircling tiny zones of necrosis. We identified no marked difference in histopathologic findings between the tumors treated with ^{99m}Tc–liposomal doxorubicin only and those that received no treatment.

Doxorubicin Quantification

Quantification of the doxorubicin extracted from the tumors revealed a close correlation ($r = 0.9185–0.9871$) between the extracted doxorubicin levels and the percentages of injected ^{99m}Tc activity in the tumor tissue, as determined at analysis of the SPECT/CT and planar scintigraphic images at all time points (Figs 5, 6). The close correlation between the extracted doxorubicin levels and the tissue counting data (Fig 7) confirmed this effect.

Discussion

The use of adjuvant chemotherapy to increase the effectiveness of thermal ablation treatment of solid tumors has been well demonstrated in animal models and with use of several drugs. In the case of RF ablation, these treatments include, in addition to liposome-encapsulated doxorubicin therapy, treatments with intravenous liposomal cisplatin (18), liposomal 5-fluorouracil (18), arsenic trioxide (20), and hydralazine (24); intravenous and intratumoral Pluronic block copolymers (28); intratumoral ethanol (11,39) and unencapsulated doxorubicin (12); intraperitoneal arsenic trioxide (20); interstitially implanted 5-fluorouracil–laden polymer rods (27); oral sorafenib (21); and transarterial chemoembolization (19,23). In human trials, the benefits of combined RF ablation–intratumoral ethanol therapy (30,40,41) and combined RF ablation–transarterial chemoembolization (15,22,25,29,31,42) have been shown.

The synergistic effect of combined RF ablation–chemotherapy has been best established with intravenous liposomal doxorubicin. Goldberg et al have shown that intravenously administered liposomal doxorubicin increases the size of the coagulation zone induced by RF ablation, as demonstrated by means of pathologic assessment in animal tumor models (13,16–18) and by means of CT follow-up in human patients (14). In a rat breast tumor model, equivalent ablation zone sizes were observed when liposomal doxorubicin was administered 3 days before to 24 hours after RF ablation (13).

Increased doxorubicin delivery to animal tumors when intravenous administration of liposomal doxorubicin is combined with RF ablation also has been well demonstrated by these investigators (16–18,32). Although all of the underlying factors are not completely understood, the mechanism of increased drug deposition seen with RF ablation is thought to be the increased microvascular permeability and inflammation caused by the thermal ablation itself. This effect is thought to be at least partially responsible for the

increased treatment effectiveness seen in these studies.

To our knowledge, the only previous demonstration of this effect at imaging was autoradiography of excised tumors that had been treated with combined RF ablation and intravenously administered tritiated liposomes (32). Our results confirm that doxorubicin delivery is increased when RF ablation is combined with the administration of the radiopharmaceutical agent ^{99m}Tc–liposomal doxorubicin, just as it is when nonradiolabeled liposomes are used, and that this can be demonstrated at noninvasive imaging over multiple time points. Furthermore, because the imaging and tissue counting results correlated closely with the drug concentration in tumors, our study results also demonstrate that the increased drug delivery that occurs with combination therapy can be not only depicted but also quantified with noninvasive imaging. This quantification could lead to a future application of imaging-based chemical dosimetry (43,44).

Given the extent of ^{99m}Tc–liposomal doxorubicin uptake identified in the tumors treated with RF ablation, it was surprising that an increase in ablation zone size at gross pathologic analysis 48 hours after treatment was not seen with this combination therapy, as compared with RF ablation alone. This may have been due to our use of a tumor model that was different from that used in previously published studies. Our model did not reveal a distinct additional outer zone of cellular necrosis at histopathologic analysis when RF ablation was performed in combination with intravenous chemotherapy, as has been described in other tumor models at the 48-hour time point (13). Despite these findings in our current research, in another study, combination therapy with RF ablation and liposomal doxorubicin in this same tumor model was significantly more effective in controlling tumor growth than was liposomal doxorubicin alone at 42 days after treatment (mean tumor size, 2.05 cm^3 ± 1.36 with combination therapy versus 5.43 cm^3 ± 0.93 with liposomal doxorubicin only) (45). It is possible that treatment-related changes
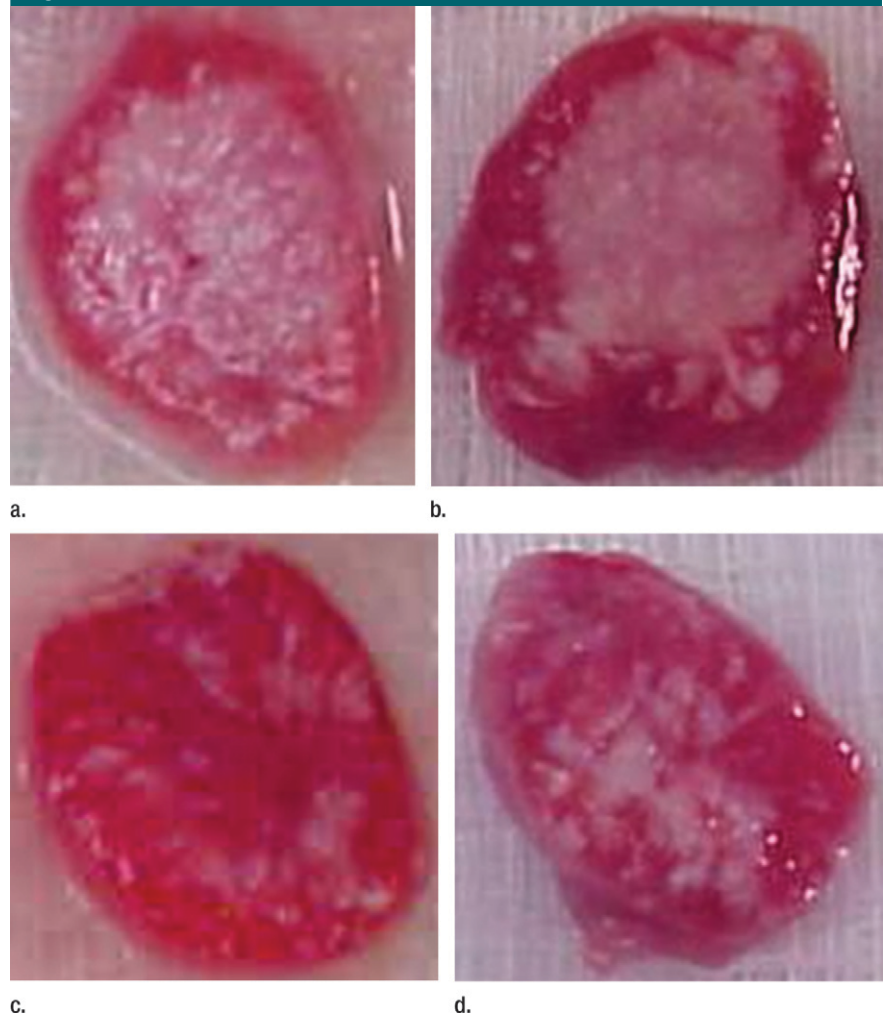
Figure 3

Figure 3:   Gross-specimen images of ablated and nonablated tumors excised and stained with triphenyltetrazolium chloride. The tumors had been treated with **(a)** combined RF ablation and intravenous ^{99m}Tc–liposomal doxorubicin, **(b)** RF ablation only, **(c)** intravenous ^{99m}Tc–liposomal doxorubicin only, or **(d)** no therapy. The ablated zones have no staining, consistent with necrosis. The tissue of the nonablated tumor in **c** and **d** is nearly completely stained, with small, scattered nonconfluent areas of spontaneous necrosis.

and the zone of ablation develop more slowly in this particular tumor model than in the other tumor models in which combination RF therapy has been investigated.

One limitation of our study was that during SPECT/CT, a contemporaneous tissue specimen was not analyzed for every imaging time point. Rather, all time points were correlated with tissue specimens obtained after the same animals were sacrificed at 44 hours after the procedure. This means that all of the SPECT/CT imaging time points

and the first three planar imaging time points were correlated with the levels of doxorubicin that eventually accumulated in those tumors. However, given that a strong correlation was seen at all time points, it may be useful to consider noncontemporaneous time points as predictive of the amount of doxorubicin that ultimately accumulates in a tumor. Furthermore, contemporaneous data from planar imaging at 44 hours and tissue counting after tumor excision confirmed the correlation between extracted doxorubicin level and tumor

radioactivity. Another potential limitation was that this study was performed in a model involving only one animal species, so the results cannot necessarily be extrapolated to other settings.

Practical applications: Combination therapy with thermal ablation and radiolabeled liposomal chemotherapy has the potential for translation to treatment of human tumors. It seems probable that the increased drug delivery confirmed in this study and in previous reports will potentiate the treatment of solid cancers in human patients. Moreover, the ability to visualize the effects of ablation over time with multimodality imaging may be of use in the noninvasive assessment of treatment response. Finally, the results suggest the future possibility of using chemodosimetry—that is, that it may be possible to use an imaging technique, such as the one described herein, to noninvasively determine the amount of drug delivered to a tumor. This capability may yield prognostic information regarding the likely success of a given tumor treatment and the possible need for repeat treatment.
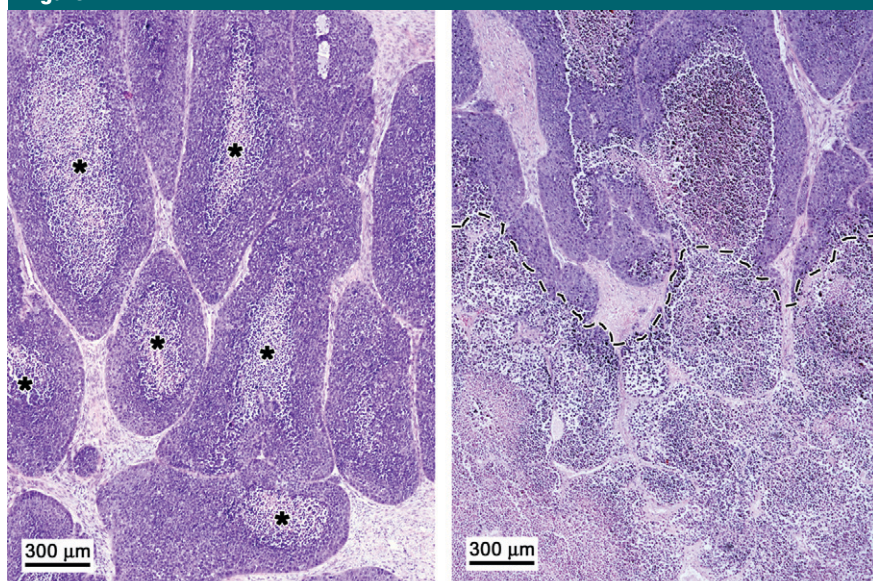
Figure 4

a.　　　　　　　b.

Figure 4: Histopathologic findings in two tumors excised from the same rat. (Hematoxylin-eosin stain; original magnification, 4×.) **(a)** Nonablated tumor specimen shows nests and cords of intact, viable tumor cells encircling a zone of necrosis (∗). **(b)** Ablated tumor specimen shows margin with nests of intact tumor cells in upper half of the specimen (above dashed line) and necrotic debris in lower half.

Figure 5

Figure 5: Graph illustrates relationship between quantity of doxorubicin (in milligrams per gram of tissue) extracted from ablated and nonablated tumors and tumoral ^{99m}Tc activity determined at analysis of SPECT/CT images acquired 20 hours after the intravenous administration of ^{99m}Tc– liposomal doxorubicin. Similar results were obtained for the 15-minute and 4-hour time points.
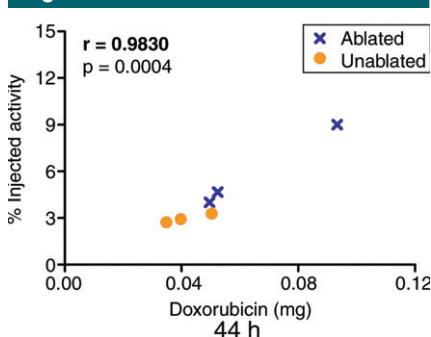
Figure 6

Figure 6: Graph illustrates relationship between quantity of doxorubicin (in milligrams per whole tumor) extracted from ablated and nonablated tumors and tumoral ^{99m}Tc activity determined at analysis of planar scintigraphic images acquired 44 hours after the intravenous administration of ^{99m}Tc–liposomal doxorubicin.
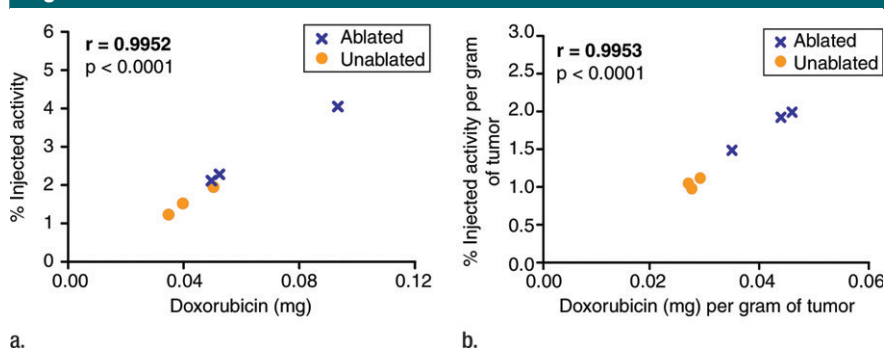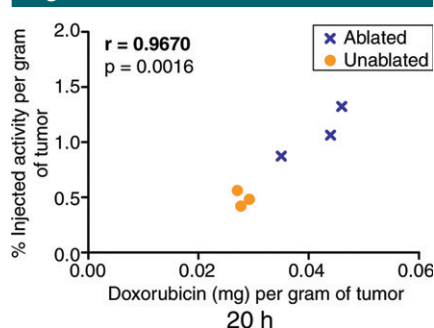
Figure 7

a.　　　　　　　b.

Figure 7: Graphs illustrate relationships between quantity of doxorubicin (in milligrams) extracted from ablated and nonablated tumors and tumoral ^{99m}Tc activity measured **(a)** per whole tumor and **(b)** per gram of tumor tissue at tissue counting in tumors excised after the intravenous administration of ^{99m}Tc–liposomal doxorubicin.

References

1. Dodd GD 3rd, Soulen MC, Kane RA, et al. Minimally invasive treatment of malignant hepatic tumors: at the threshold of a major breakthrough. RadioGraphics 2000;20(1):9–27.

2. Gillams AR. Thermal ablation of liver metastases. Abdom Imaging 2001;26(4): 361–368.

3. Head HW, Dodd GD 3rd. Thermal ablation for hepatocellular carcinoma. Gastroenterology 2004;127(5,Suppl 1):S167–S178.

4. Hinshaw JL, Lee FT Jr. Image-guided ablation of renal cell carcinoma. Magn Reson Imaging Clin N Am 2004;12(3):429–447, vi.

5. Krehbiel K, Ahmad A, Leyendecker J, Zagoria R. Thermal ablation: update and technique at a high-volume institution. Abdom Imaging 2008;33(6):695–706.

6. McTaggart RA, Dupuy DE. Thermal ablation of lung tumors. Tech Vasc Interv Radiol 2007;10(2):102–113.

7. Simon CJ, Dupuy DE. Percutaneous minimally invasive therapies in the treatment of bone tumors: thermal ablation. Semin Musculoskelet Radiol 2006;10(2):137–144.

8. Moser T, Buy X, Goyault G, Tok CH, Irani F, Gangi A. Image-guided ablation of bone tumors: review of current techniques [in French]. J Radiol 2008;89(4):461–471.

9. Huston TL, Simmons RM. Ablative therapies for the treatment of malignant diseases of the breast. Am J Surg 2005;189(6): 694–701.

10. van Esser S, van den Bosch MA, van Diest PJ, Mali WT, Borel Rinkes IH, van Hillegersberg R. Minimally invasive ablative therapies for invasive breast carcinomas: an overview of current literature. World J Surg 2007;31(12):2284–2292.

11. Goldberg SN, Kruskal JB, Oliver BS, Clouse ME, Gazelle GS. Percutaneous tumor ablation: increased coagulation by combining radio-frequency ablation and ethanol instillation in a rat breast tumor model. Radiology 2000;217(3):827–831.

12. Goldberg SN, Saldinger PF, Gazelle GS, et al. Percutaneous tumor ablation: increased necrosis with combined radio-frequency ablation and intratumoral doxorubicin injection in a rat breast tumor model. Radiology 2001;220(2):420–427.

13. Goldberg SN, Girnan GD, Lukyanov AN, et al. Percutaneous tumor ablation: increased necrosis with combined radio-frequency ablation and intravenous liposomal doxorubicin in a rat breast tumor model. Radiology 2002;222(3):797–804.

14. Goldberg SN, Kamel IR, Kruskal JB, et al. Radiofrequency ablation of hepatic tumors: increased tumor destruction with adjuvant liposomal doxorubicin therapy. AJR Am J Roentgenol 2002;179(1):93–101.

15. Kitamoto M, Imagawa M, Yamada H, et al. Radiofrequency ablation in the treatment of small hepatocellular carcinomas: comparison of the radiofrequency effect with and without chemoembolization. AJR Am J Roentgenol 2003;181(4):997–1003.

16. Ahmed M, Monsky WE, Girnun G, et al. Radiofrequency thermal ablation sharply increases intratumoral liposomal doxorubicin accumulation and tumor coagulation. Cancer Res 2003;63(19):6327–6333.

17. Ahmed M, Liu Z, Lukyanov AN, et al. Combination radiofrequency ablation with intratumoral liposomal doxorubicin: effect on drug accumulation and coagulation in multiple tissues and tumor types in animals. Radiology 2005;235(2):469–477.

18. Ahmed M, Lukyanov AN, Torchilin V, Tournier H, Schneider AN, Goldberg SN. Combined radiofrequency ablation and adjuvant liposomal chemotherapy: effect of chemotherapeutic agent, nanoparticle size, and circulation time. J Vasc Interv Radiol 2005;16(10):1365–1371.

19. Sugimori K, Nozawa A, Morimoto M, et al. Extension of radiofrequency ablation of the liver by transcatheter arterial embolization with iodized oil and gelatin sponge: results in a pig model. J Vasc Interv Radiol 2005;16(6):849–856.

20. Hines-Peralta A, Sukhatme V, Regan M, Signoretti S, Liu ZJ, Goldberg SN. Improved tumor destruction with arsenic trioxide and radiofrequency ablation in three animal models. Radiology 2006;240(1): 82–89.

21. Hakimé A, Hines-Peralta A, Peddi H, et al. Combination of radiofrequency ablation with antiangiogenic therapy for tumor ablation efficacy: study in mice. Radiology 2007;244(2):464–470.

22. Shiraishi R, Yamasaki T, Saeki I, et al. Pilot study of combination therapy with transcatheter arterial infusion chemotherapy using iodized oil and percutaneous radiofrequency ablation during occlusion of hepatic blood flow for hepatocellular carcinoma. Am J Clin Oncol 2008;31(4): 311–316.

23. Mostafa EM, Ganguli S, Faintuch S, Mertyna P, Goldberg SN. Optimal strategies for combining transcatheter arterial chemoembolization and radiofrequency ablation in rabbit VX2 hepatic tumors. J Vasc Interv Radiol 2008;19(12):1740–1748.

24. Wu H, Exner AA, Krupka TM, Weinberg BD, Haaga JR. Vasomodulation of tumor blood flow: effect on perfusion and thermal ablation size. Ann Biomed Eng 2009;37(3): 552–564.

25. Yamakado K, Nakatsuka A, Ohmori S, et al. Radiofrequency ablation combined with chemoembolization in hepatocellular carcinoma: treatment response based on tumor size and morphology. J Vasc Interv Radiol 2002;13(12):1225–1232.

26. D'Ippolito G, Ahmed M, Girnun GD, et al. Percutaneous tumor ablation: reduced tumor growth with combined radio-frequency ablation and liposomal doxorubicin in a rat breast tumor model. Radiology 2003; 228(1):112–118.

27. Haaga JR, Exner AA, Wang Y, Stowe NT, Tarcha PJ. Combined tumor therapy by using radiofrequency ablation and 5-FU–laden polymer implants: evaluation in rats and rabbits. Radiology 2005;237(3):911–918.

28. Weinberg BD, Krupka TM, Haaga JR, Exner AA. Combination of sensitizing pretreatment and radiofrequency tumor ablation: evaluation in rat model. Radiology 2008;246(3):796–803.

29. Yamakado K, Nakatsuka A, Kobayashi S, et al. Radiofrequency ablation combined with renal arterial embolization for the treatment of unresectable renal cell carcinoma larger than 3.5 cm: initial experience. Cardiovasc Intervent Radiol 2006;29(3): 389–394.

30. Zhang YJ, Liang HH, Chen MS, et al. Hepatocellular carcinoma treated with radiofrequency ablation with or without ethanol injection: a prospective randomized trial. Radiology 2007;244(2):599–607.

31. Cheng BQ, Jia CQ, Liu CT, et al. Chemoembolization combined with radiofrequency ablation for patients with hepatocellular carcinoma larger than 3 cm: a randomized controlled trial. JAMA 2008;299(14):1669–1677.

32. Monsky WL, Kruskal JB, Lukyanov AN, et al. Radio-frequency ablation increases intratumoral liposomal doxorubicin accumulation in a rat breast tumor model. Radiology 2002;224(3):823–829.

33. Institute of Laboratory Animal Resources, Commission on Life Sciences, National Research Council. Guide for the care and use

Radiology

of laboratory animals. Washington, DC: National Academy Press, 1996.

34. Bao A, Phillips WT, Goins B, et al. Setup and characterization of a human head and neck squamous cell carcinoma xenograft model in nude rats. Otolaryngol Head Neck Surg 2006;135(6):853–857.

35. Bao A, Goins B, Klipper R, Negrete G, Phillips WT. Direct 99mTc labeling of pegylated liposomal doxorubicin (Doxil) for pharmacokinetic and non-invasive imaging studies. J Pharmacol Exp Ther 2004;308(2):419–425.

36. Bao A, Phillips WT, Goins B, et al. Potential use of drug carried-liposomes for cancer therapy via direct intratumoral injection. Int J Pharm 2006;316(1-2):162–169.

37. Gabizon A, Shmeeda H, Barenholz Y. Pharmacokinetics of pegylated liposomal doxorubicin: review of animal and human studies. Clin Pharmacokinet 2003;42(5):419–436.

38. Bederson JB, Pitts LH, Germano SM, Nishimura MC, Davis RL, Bartkowski HM. Evaluation of 2,3,5-triphenyltetrazolium chloride as a stain for detection and quanti-fication of experimental cerebral infarction in rats. Stroke 1986;17(6):1304–1308.

39. Frieser M, Schaber S, Strobel D, et al. Prolonged survival through combined treatment with radiofrequency ablation/ethanol instillation compared with radiofrequency ablation alone in the VX2 rabbit liver tumour model [in German]. Ultraschall Med 2007;28(2):176–180.

40. Akhlaghpoor S, Tomasian A, Arjmand Shabestari A, Ebrahimi M, Alinaghizadeh MR. Percutaneous osteoid osteoma treatment with combination of radiofrequency and alcohol ablation. Clin Radiol 2007; 62(3):268–273.

41. Wong SN, Lin CJ, Lin CC, Chen WT, Cua IH, Lin SM. Combined percutaneous radiofrequency ablation and ethanol injection for hepatocellular carcinoma in high-risk locations. AJR Am J Roentgenol 2008;190(3):W187–W195.

42. Wang YB, Chen MH, Yan K, Yang W, Dai Y, Yin SS. Quality of life after radiofrequency ablation combined with transcatheter arterial chemoembolization for hepatocellular carcinoma: comparison with transcatheter arterial chemoembolization alone. Qual Life Res 2007;16(3):389–397.

43. Kleiter MM, Yu D, Mohammadian LA, et al. A tracer dose of technetium-99m-labeled liposomes can estimate the effect of hyperthermia on intratumoral doxil extravasation. Clin Cancer Res 2006;12(22): 6800–6807.

44. Tashjian JA, Dewhirst MW, Needham D, Viglianti BL. Rationale for and measurement of liposomal drug delivery with hyperthermia using non-invasive imaging techniques. Int J Hyperthermia 2008; 24(1):79–90.

45. Soundararajan A, Bao A, Phillips WT, Dodd GD 3rd, Goins BA. Chemo-radionuclide therapy with rhenium-186 labeled liposomal doxorubicin in combination with radiofrequency ablation for effective treatment of head and neck cancer [abstr]. In: Radiological Society of North America scientific assembly and annual meeting program. Oak Brook, Ill: Radiological Society of North America, 2008; 308.